NASA TN D-145

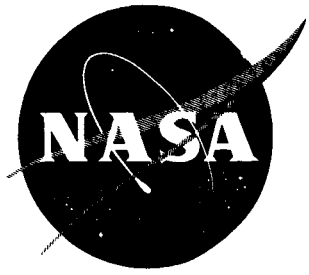

TECHNICAL NOTE

D-145

WATER-LANDING IMPACT ACCELERATIONS FOR

THREE MODELS OF REENTRY CAPSULES

By Victor L. Vaughan, Jr.

Langley Research Center
Langley Field, Va.

NATIONAL AERONAUTICS AND SPACE ADMINISTRATION

WASHINGTON

October 1959

NATIONAL AERONAUTICS AND SPACE ADMINISTRATION

TECHNICAL NOTE D-145

WATER-LANDING IMPACT ACCELERATIONS FOR THREE MODELS OF REENTRY CAPSULES

By Victor L. Vaughan, Jr.

SUMMARY

Experimental investigations have been conducted to determine the rigid-body impact accelerations for three models of reentry capsules during simulated parachute-supported water landings. The main bodies of the models were conical in shape. Two of the models were 1/12 scale; one had a segment of a sphere as a bottom and the other had a 53° conical shape as a bottom. The third model was 1/6 scale and had a convex-concave bottom. The models were tested for nominal flight paths of 90° (vertical) and 65° to simulate parachute landings with no wind and with wind, respectively, and nominal contact attitudes of ±30°, ±15°, and 0° to simulate attitudes that might occur as a result of swinging of the capsule under the parachute. Accelerations of the models at impact were measured along the X (roll) and Z (yaw) axes by accelerometers installed at the centers of gravity.

The maximum accelerations along the X-axis for the three forms were higher for inclined flight-path angles than for the vertical flight path, and varied as the square of the vertical contact velocity for a given shape, flight path, attitude, and mass. The maximum accelerations along the X-axis for the model with the spherical bottom were about 50g at a contact attitude of 0° and dropped sharply to about 10g with increase in contact attitude to about ±30°. The maximum accelerations for the model with the conical bottom were about 10g and were independent of contact attitude.

The accelerations along the Z-axis were small for the models with the spherical and conical bottoms at a contact attitude of 0° regardless of flight-path angle and small (up to 3g) for the model with the spherical bottom for all test conditions. The accelerations increased along the Z-axis of the model with the conical bottom to about 11g with departure from the 0° attitude condition.

The maximum accelerations along the X-axis of the model with the convex-concave bottom were about 17g at a contact attitude of 0° and increased to about 28g with increase in contact attitude to ±30°. The accelerations along the Z-axis were small at a contact attitude of 0° for the model with the convex-concave bottom and increased to about 13g at a ±30° contact attitude.

INTRODUCTION

Interest has recently been shown in obtaining information on the impact accelerations which might occur on reentry capsules during parachute-supported water landings. In this connection, experimental investigations have been made by the Langley Research Center to determine water-landing impact accelerations on models of conical-shaped reentry capsules having a variety of impact bottoms. One such model had a segment of a sphere for a bottom which was designed to serve as a heat shield upon reentry into the atmosphere. A full-scale reentry capsule of this configuration has been tested and is reported with some of the present model data in reference 1. Another model had a 53° conical bottom which was also designed to serve as a heat shield. The third model was designed for low accelerations on water impact and had a convex-concave bottom. This bottom shape has not been developed as a heat shield but could be used as a second bottom that would be exposed for landing purposes by dropping the heat shield from the capsule.

Since the final descent of the capsule to a water landing would be by means of a parachute, some of the effects of surface winds were simulated by using various flight paths. A range of contact attitudes was tested to simulate the attitudes that might occur if the capsule were swinging under the parachute at water contact. A wide range of vertical contact velocities was investigated to determine the effects of velocity on impact accelerations.

MODEL DESCRIPTIONS

Drawings of the three models of reentry capsules with full-scale dimensions are shown in figure 1. The dynamic models were constructed of fiber glass and plastic and the construction was as rigid as possible to eliminate structural vibrations. For purposes of identification the models have been designated as models A, B, and C.

Model A was 1/12 scale and had a segment of a sphere as a bottom. The model had a full-scale weight of 2,270 pounds. This is the same model for which data are reported in reference 1.

Model B was 1/12 scale and had a 53° conical shape as a bottom. The model had a full-scale weight of 2,000 pounds.

Model C was 1/6 scale and had a convex-concave bottom. This bottom was designed, by use of the computation procedure outlined in reference 1, to have a rate of application of acceleration upon water contact of about 500g per second and a maximum acceleration of 15g. The other design

parameters were a vertical flight path, 0° contact attitude, and a full-scale vertical contact velocity of 30 feet per second and weight of 1,000 pounds.

APPARATUS AND PROCEDURE

Two strain-gage-type accelerometers were located at the center of gravity of each model and rigidly attached to the bottom of the model. The accelerometers were capable of recording accelerations of 200g and 25g along the X-axis and Z-axis, respectively. A drawing showing the axis system of the models is presented in figure 2. The signals from the accelerometers were transmitted through cables to amplifying and recording equipment. The natural frequency of the 200g accelerometer was about 900 cycles per second and that of the 25g accelerometer was about 350 cycles per second. The accelerometers were damped to 65 percent of critical damping. The response of the recording equipment was flat to about 2,200 cycles per second.

Nominal flight paths of 90° (vertical) and 65° and a range of contact attitudes from -30° to 30° were investigated. The flight paths and contact attitudes are identified in figure 2. The tests for the vertical flight path were made by a free-fall method, the models being dropped from the required heights to obtain the range of speeds from 10 to 45 feet per second at water contact. The tests for the 65° flight path were conducted with a catapult type of test apparatus as shown in figure 3. The catapult consisted of a steel staff which followed the flight path by moving through a rigidly mounted roller cage. A yoke, which held the model by means of pins inserted into sleeves at the edge of the model base, was mounted at the bottom of the staff. The pins were under spring tension and were retracted at the end of the catapult stroke to free the model. The desired attitude was set by a sting which was fixed to the staff and inserted into the top of the model. Desired speeds were obtained by varying the catapult stroke or by using a shock-cord drive. The velocity of the catapult was measured by recording the time for the staff to travel the last 2 inches of the catapult stroke. An electronic counter, capable of recording time to 1/100,000 of a second, was used for this purpose. The catapult velocity was combined with the velocity computed for the free-fall height, which was the height between the model release point and the water surface, to obtain the actual contact velocity.

Most of the tests for the 90° and 65° flight paths were made at a full-scale vertical contact velocity of 30 feet per second with a variation of ±1.5 feet per second. The other velocities were investigated to determine the effects of velocity on impact accelerations. The flight paths and contact attitudes of the models were recorded by a high-speed

motion-picture camera. The nominal 65° flight path varied from 65° to 69°. The tests were conducted in calm water in the Langley tank. The density of the water was 1.94 slugs/cu ft.

RESULTS AND DISCUSSION

Typical time histories of accelerations along the X- and Z-axes for the three models are presented in figures 4 and 5. Maximum accelerations are plotted against contact attitude for the three models in figures 6 to 11. All values shown are full scale.

The maximum accelerations along the X-axis for model A (fig. 6) were about 40g for a contact attitude of 0° and a vertical flight path at a vertical contact velocity of approximately 30 feet per second. For the 65° flight path, 0° contact attitude, and 30-feet-per-second vertical contact velocity the maximum accelerations were about 50g. The increase in accelerations due to the change to a 65° flight path was caused by the increased velocity along the 65° flight path as compared with the velocity along the vertical flight path. Increase in vertical contact velocity to approximately 38 feet per second for the 65° flight path and 0° contact attitude increased the accelerations to about 80g. Increase in contact attitude in either the positive or negative direction from 0° reduced the accelerations until at ±30° attitude the accelerations were about 10g for both flight paths. The lower accelerations may be attributed to the wedge shape of the impact surface at 30° attitude as compared with the blunt impact surface at 0° attitude.

The maximum accelerations along the Z-axis for model A are shown in figure 7. There were no measurable accelerations along the Z-axis for either flight path at a contact attitude of 0° and a vertical contact velocity of approximately 30 feet per second. The increase in contact attitude from 0° to about 30° caused very small accelerations, about 2g, for a vertical flight path. Increase in contact attitude in the negative direction from 0° to 30° attitude for the 65° flight path gave accelerations of about 3g or 4g. The same values of acceleration were obtained for positive attitudes; however, the direction of the accelerations along the Z-axis was reversed. Increase in the vertical contact velocity to approximately 38 feet per second had a negligible effect on the accelerations along the Z-axis throughout the full range of contact attitudes.

Maximum accelerations along the X-axis of model B for a vertical contact velocity of approximately 30 feet per second are shown in figure 8, with data for model A as a reference. The difference in weights between models A and B is 13 percent, and check tests indicated that for a vertical flight path and a contact attitude of 0° the weight

difference caused a very small (3g) variation in the maximum acceleration. This was substantiated by calculations using the computation procedure outlined in reference 1. Figure 8 shows that the accelerations along the X-axis for model B were about 10g for both flight paths at a contact attitude of 0°. The lower accelerations of model B as compared with model A may be attributed to the more pointed impact surface of the conical-shaped bottom of model B. Increase in contact attitude in either the positive or negative direction from 0° to 30° had very little effect on the accelerations along the X-axis of model B for both flight paths. It may be noted that the accelerations at 30° contact attitude were about the same for models A and B.

Maximum accelerations along the Z-axis of model B at a vertical contact velocity of 30 feet per second are shown in figure 9, with data for model A as a reference. There were no measurable accelerations along the Z-axis of model B at a contact attitude of 0° for a vertical flight path. The increase in contact attitude from 0° to 30° gave accelerations of about 7g for a vertical flight path. There were very small accelerations, about 2g to 3g, along the Z-axis of model B at a contact attitude of 0° and a 65° flight path. Increases in the contact attitude in the negative direction from 0° to 30° increased the accelerations to about 11g. Increases in the contact attitude in the positive direction from 0° to 30° increased the accelerations along the Z-axis to about 8g.

Comparisons between model C and models A and B have not been made because of the difference in design parameters between the models.

Maximum accelerations along the X-axis of model C for a vertical contact velocity of approximately 30 feet per second are shown in figure 10. The accelerations along the X-axis at a contact attitude of 0° were about 17g for both flight paths with a rate of application of acceleration of about 400g per second. This compares very closely with the 500g per second rate of application of acceleration and the maximum of 15g for which the model was designed. Increase in contact attitude in either the positive or negative direction from 0° increased the accelerations along the X-axis until at ±30° attitude the accelerations were about 28g for both flight paths.

Maximum accelerations along the Z-axis of model C at a vertical contact velocity of 30 feet per second are shown in figure 11. There were no accelerations along the Z-axis of model C at a contact attitude of 0° for a vertical flight path. The increase in contact attitude from 0° to 30° gave accelerations of about 15g for a vertical flight path. There were very small accelerations, about 2g to 3g, along the Z-axis of model C at a contact attitude of 0° and a 65° flight path. Increase in contact attitude in the negative direction from 0° to 30° increased the accelerations to about 13g. Increase in contact attitude

in the positive direction from 0° to 30° increased the accelerations along the Z-axis of model C to about 11g.

The effects of vertical contact velocity on the accelerations along the X-axis of models A, B, and C at a contact attitude of 0° are presented in figure 12. The scale along the abscissa of figure 12 is proportional to the square of the velocity. Within the limits of the investigation, for a given shape, flight-path angle, attitude, and mass, the accelerations along the X-axis increased directly as the square of the vertical contact velocity. This statement also applies for velocities along the flight path. A linear variation in acceleration with the square of the velocity is expected from the fact that displacement at any given instant is the same regardless of contact velocity, provided all other parameters are invariant. Calculations by means of the computation procedure outlined in reference 1 verify the results given in figure 12.

Sequence photographs showing a typical landing of model A from a 65° flight path at a -30° contact attitude and a vertical contact velocity of 30 feet per second are shown in figure 13. At 0.01 second after contact the model penetration is very small with a negligible change in attitude. As the penetration increases the model changes attitude in a positive direction, and at 0.48 second after contact it has reached maximum penetration and attitude change.

Sequence photographs of a landing for model C from a 65° flight path at a -30° contact attitude and a vertical velocity of 30 feet per second are shown in figure 14. The motions of the model are very similar to those of model A. Maximum penetration and attitude change occur at 0.44 second after contact. The force of buoyancy and the force of the following wave, which strikes the back of the model, causes the model to recover rapidly so that at 0.97 second after contact the model has rebounded to a position above the water surface.

CONCLUDING REMARKS

In general, the maximum accelerations along the X-axis of the three models for a given vertical contact velocity were higher for inclined flight-path angles than for the vertical flight path. For a given shape, flight path, altitude, and mass the accelerations varied as the square of the vertical contact velocity.

At a contact attitude of 0° the maximum accelerations were 50g for the model with the spherical bottom and 10g for the model with the conical bottom. Increase in contact attitude in either the positive or negative direction resulted in a reduction in acceleration to about 10g

at a 30° attitude for the model with the spherical bottom, while the increase in contact attitude had little effect on the model with the conical bottom.

The maximum accelerations along the Z-axis were small at a contact attitude of 0° for the models with the spherical and the conical bottoms and small (up to 3g) for the model with the spherical bottom for all test conditions. The accelerations along the Z-axis increased to about 11g at a 30° contact attitude for the model with the conical bottom.

L
5
4
0

The maximum accelerations along the X-axis of the model with the convex-concave bottom were about 17g at a contact attitude of 0° and increased to about 28g with increase in contact attitude to ±30° attitude. The accelerations along the Z-axis were small at a contact attitude of 0° for the model with the convex-concave bottom and increased to about 13g at a ±30° contact attitude.

Langley Research Center,
National Aeronautics and Space Administration,
Langley Field, Va., July 30, 1959.

REFERENCE

1. McGehee, John R., Hathaway, Melvin E., and Vaughan, Victor L., Jr.: Water-Landing Characteristics of a Reentry Capsule. NASA MEMO 5-23-59L, 1959.

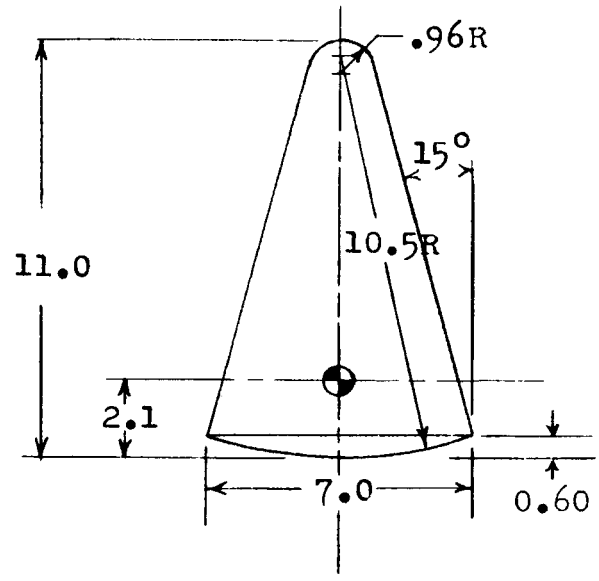

Model A (Spherical bottom)

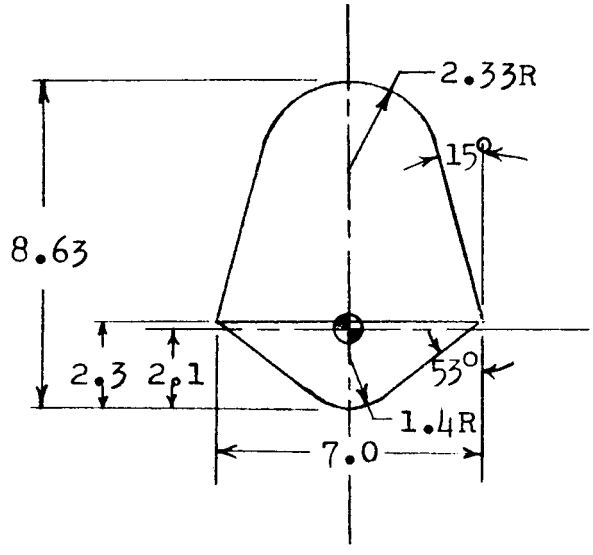

Model B (Conical bottom)

Figure 1.- Details of models. Dimensions are full scale in feet.

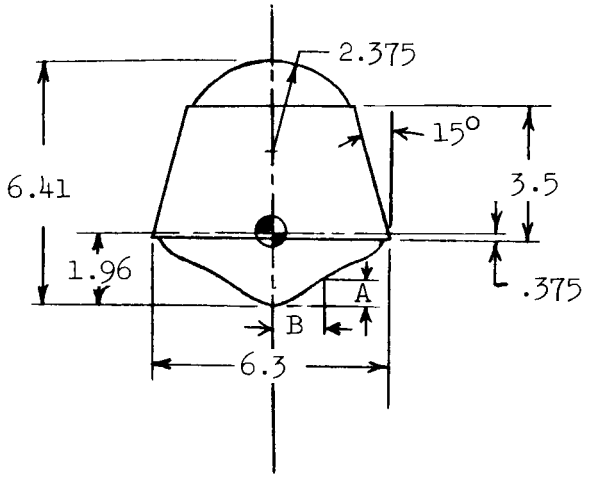

Model C (convex-concave bottom)

Bottom Coordinates	
A	B
0	0
.030	.138
.119	.350
.296	.654
.440	.863
.577	1.063
.705	1.263
.825	1.470
.926	1.680
1.018	1.890
1.100	2.110
1.172	2.340
1.250	2.525
1.500	2.830
1.750	2.965
2.000	3.000

Figure 1.- Concluded.

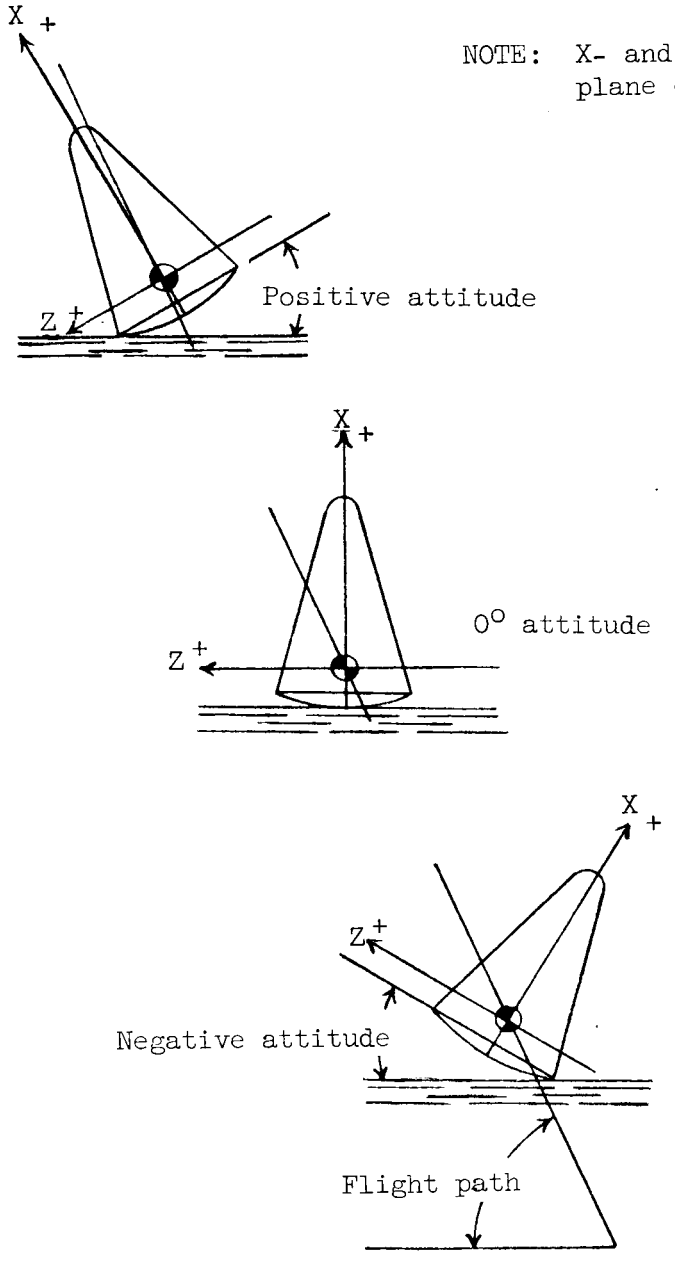

Figure 2.- Drawings identifying axes, force directions, flight paths, and contact attitudes.

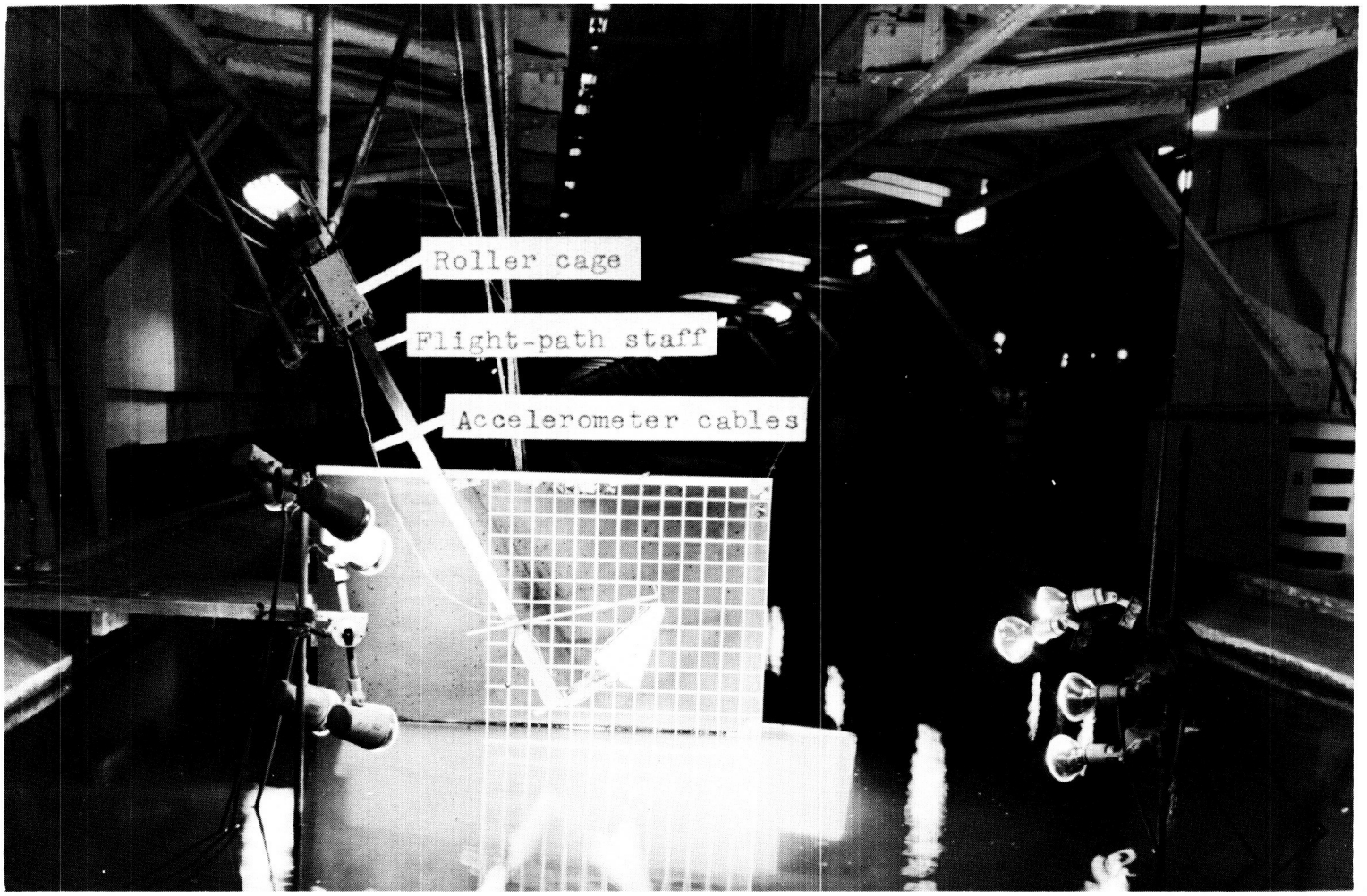

Figure 3.- Model test setup. L-59-5014

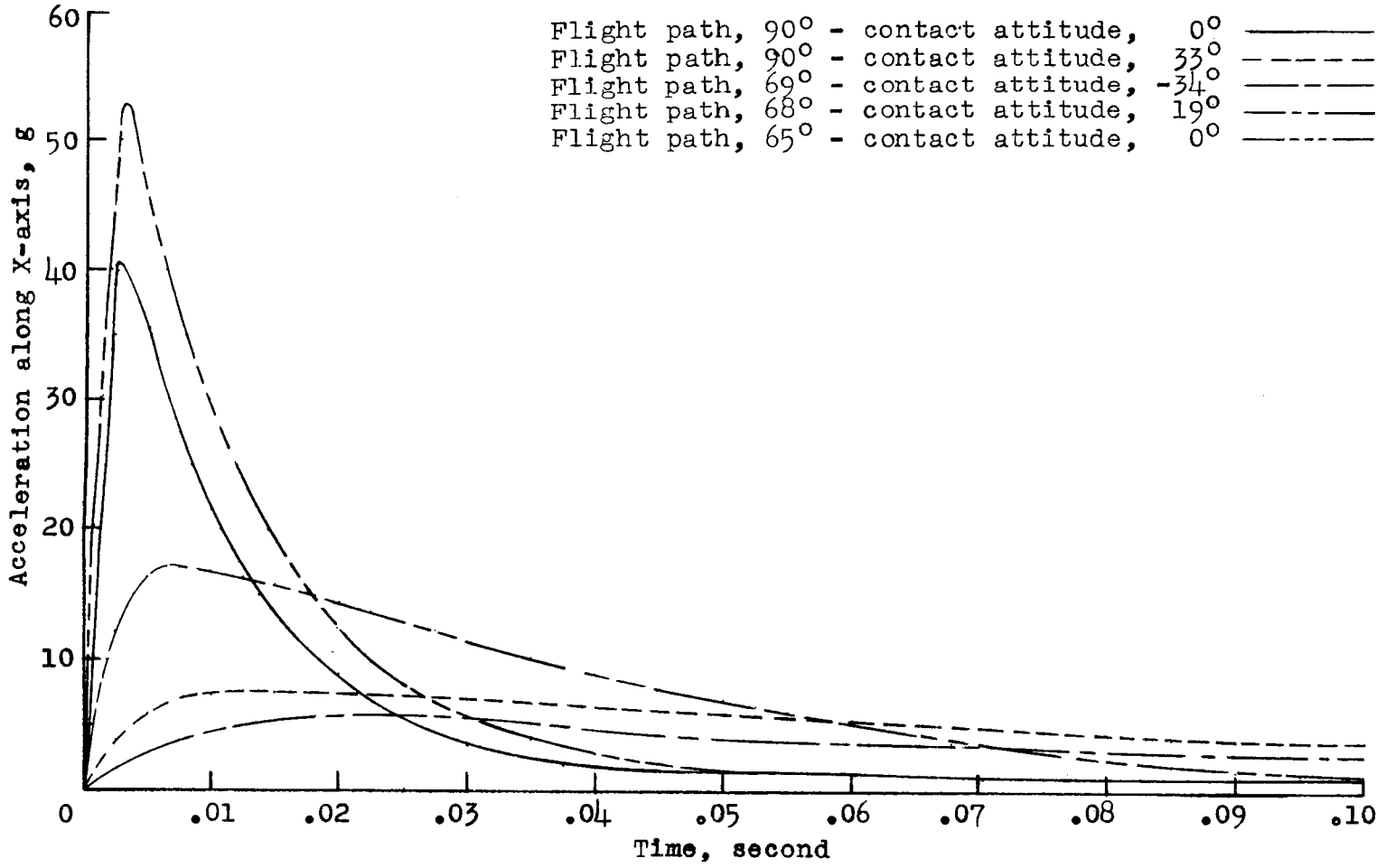

(a) Model A.

Figure 4.- Typical time histories of accelerations along the X-axis at a contact velocity of 30 feet per second. All values are full scale.

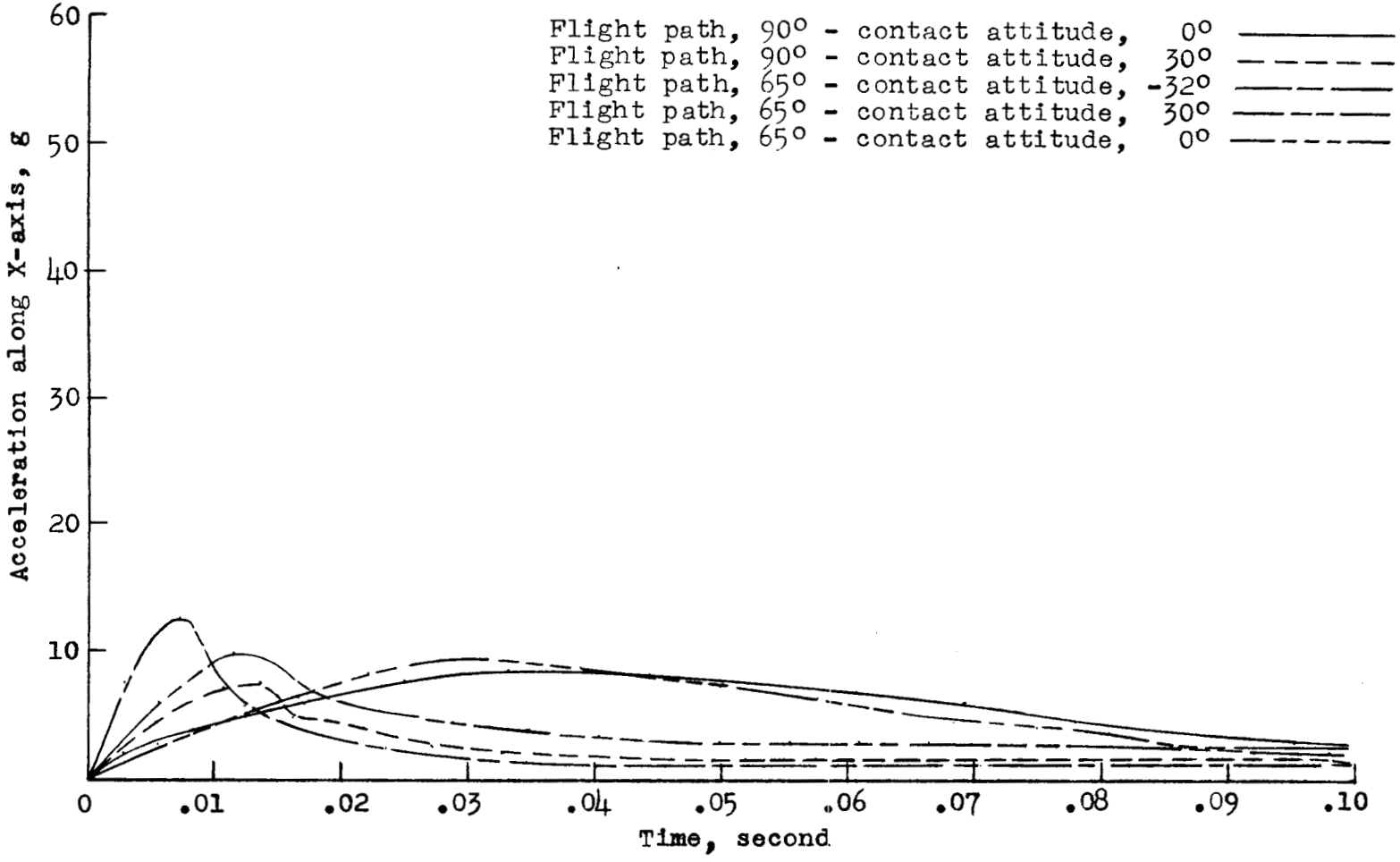

(b) Model B.

Figure 4.- Continued.

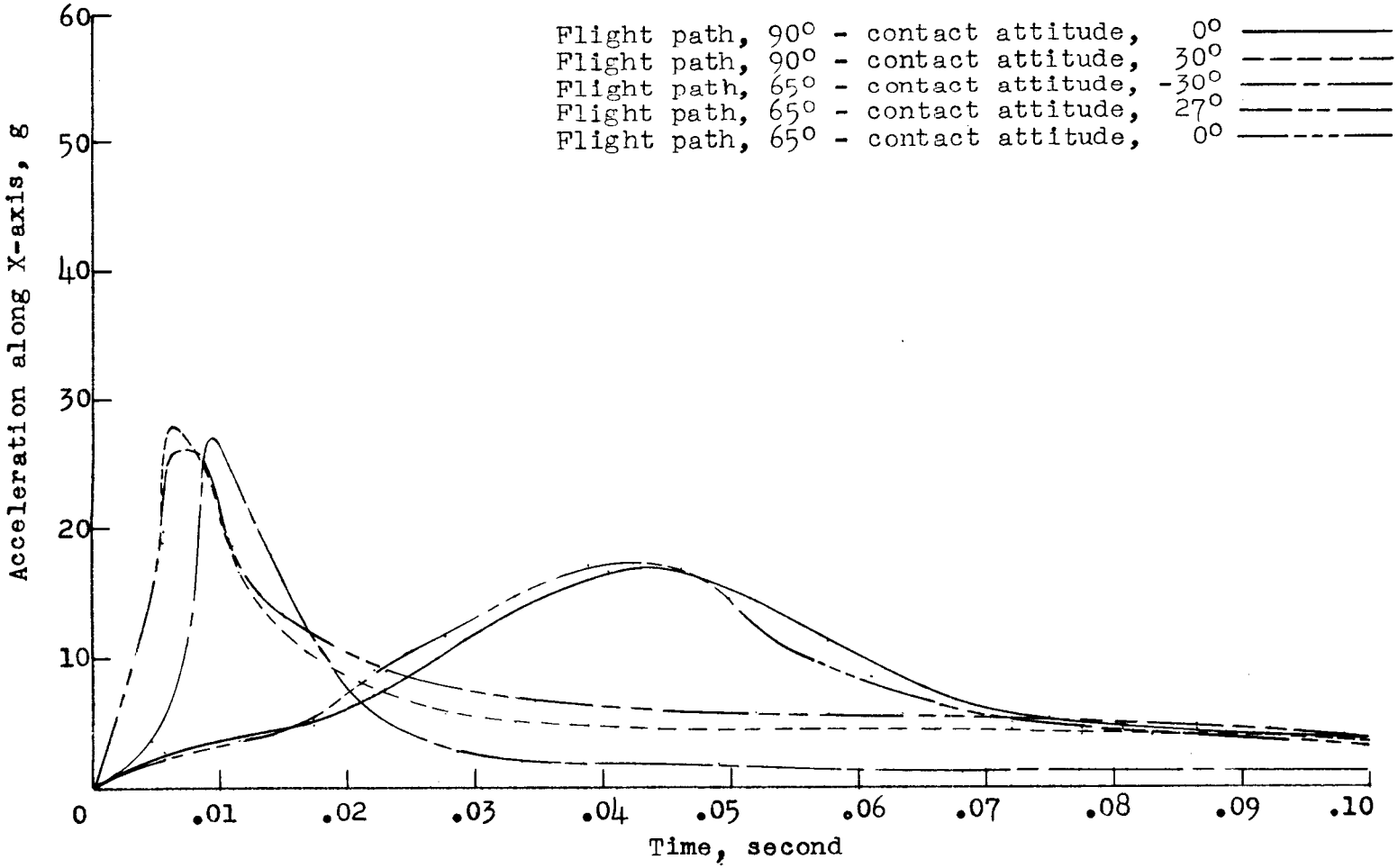

(c) Model C.

Figure 4.- Concluded.

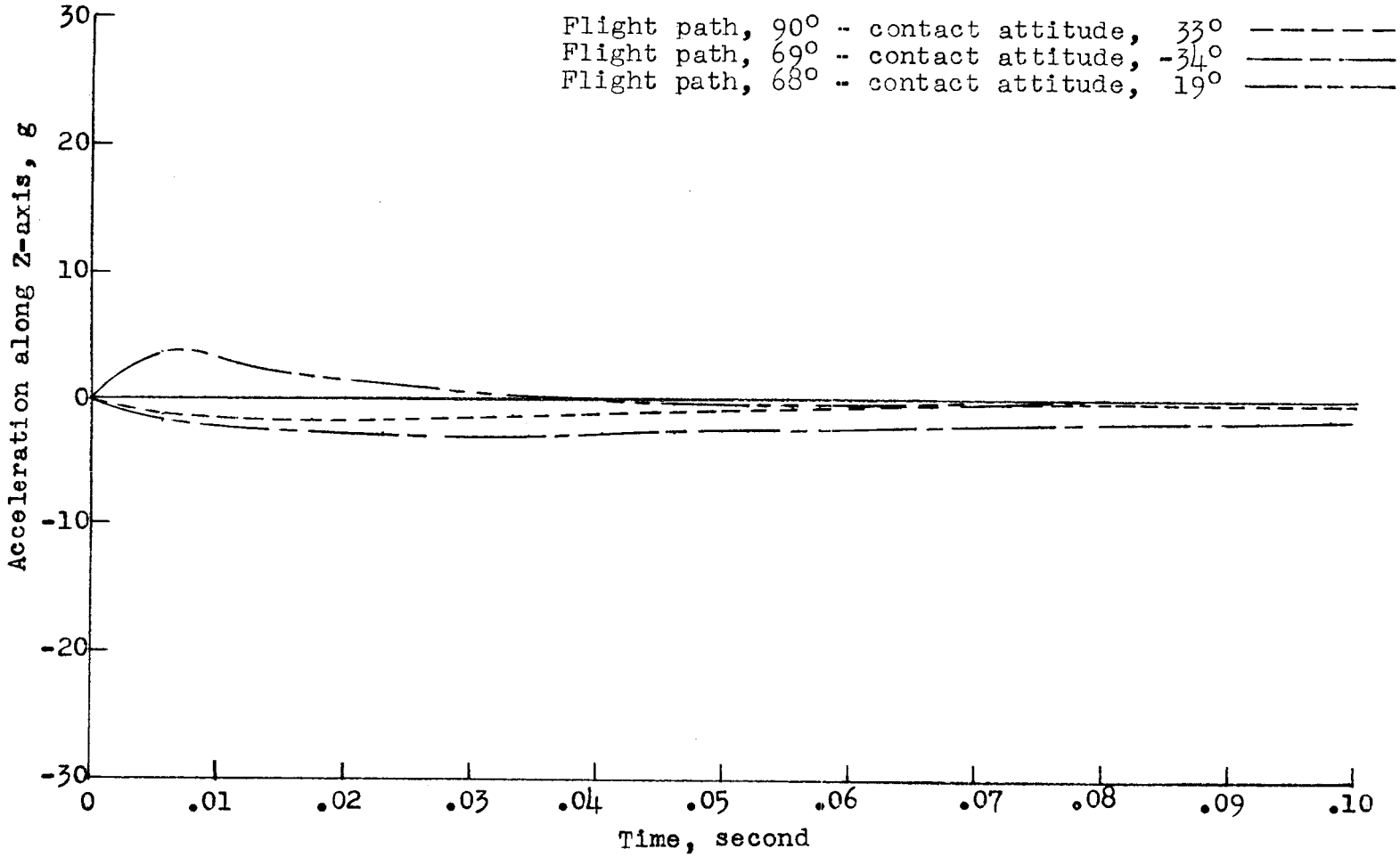

(a) Model A.

Figure 5.- Typical time histories of accelerations along the Z-axis at a contact velocity of 30 feet per second. All values are full scale.

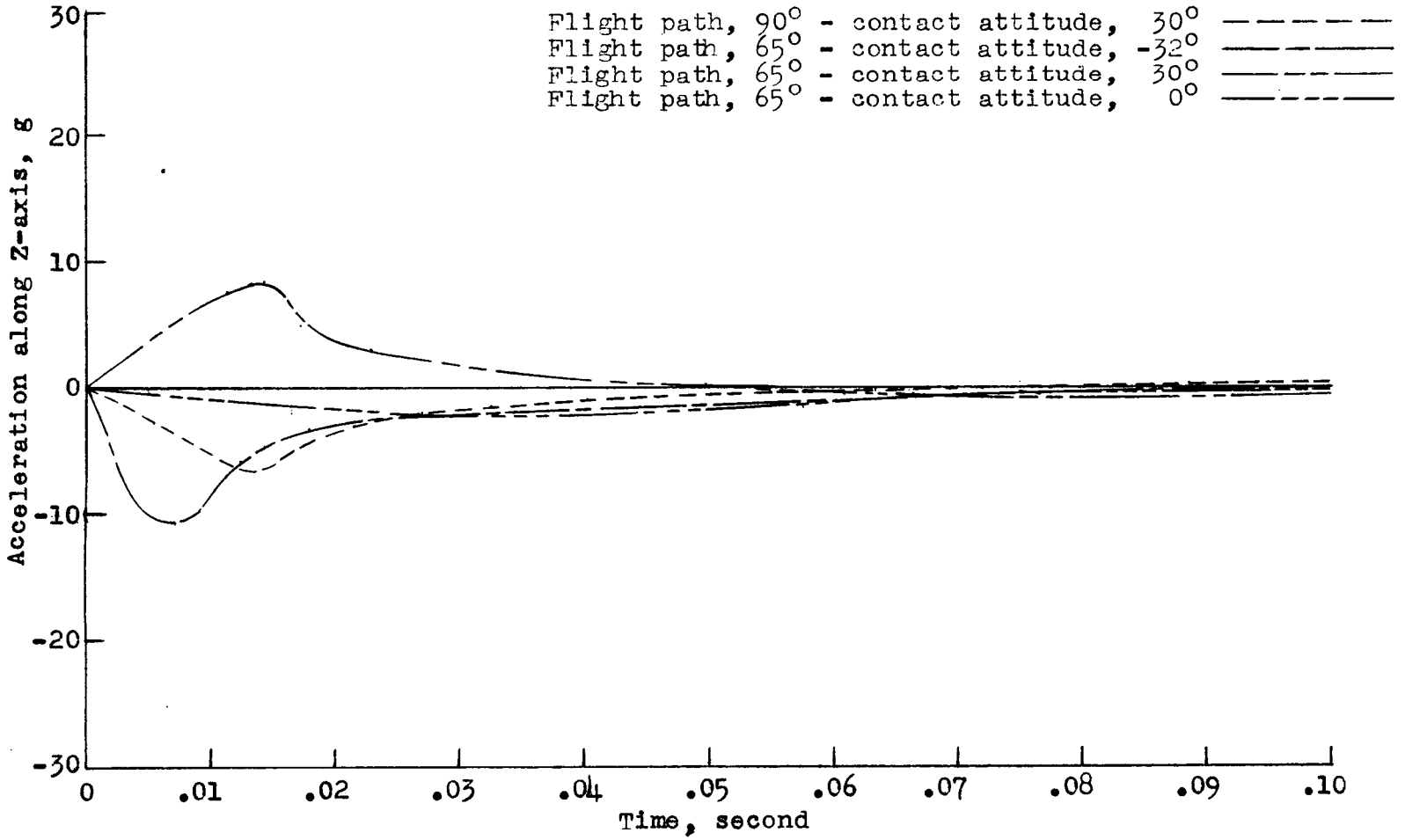

(b) Model B.

Figure 5.- Continued.

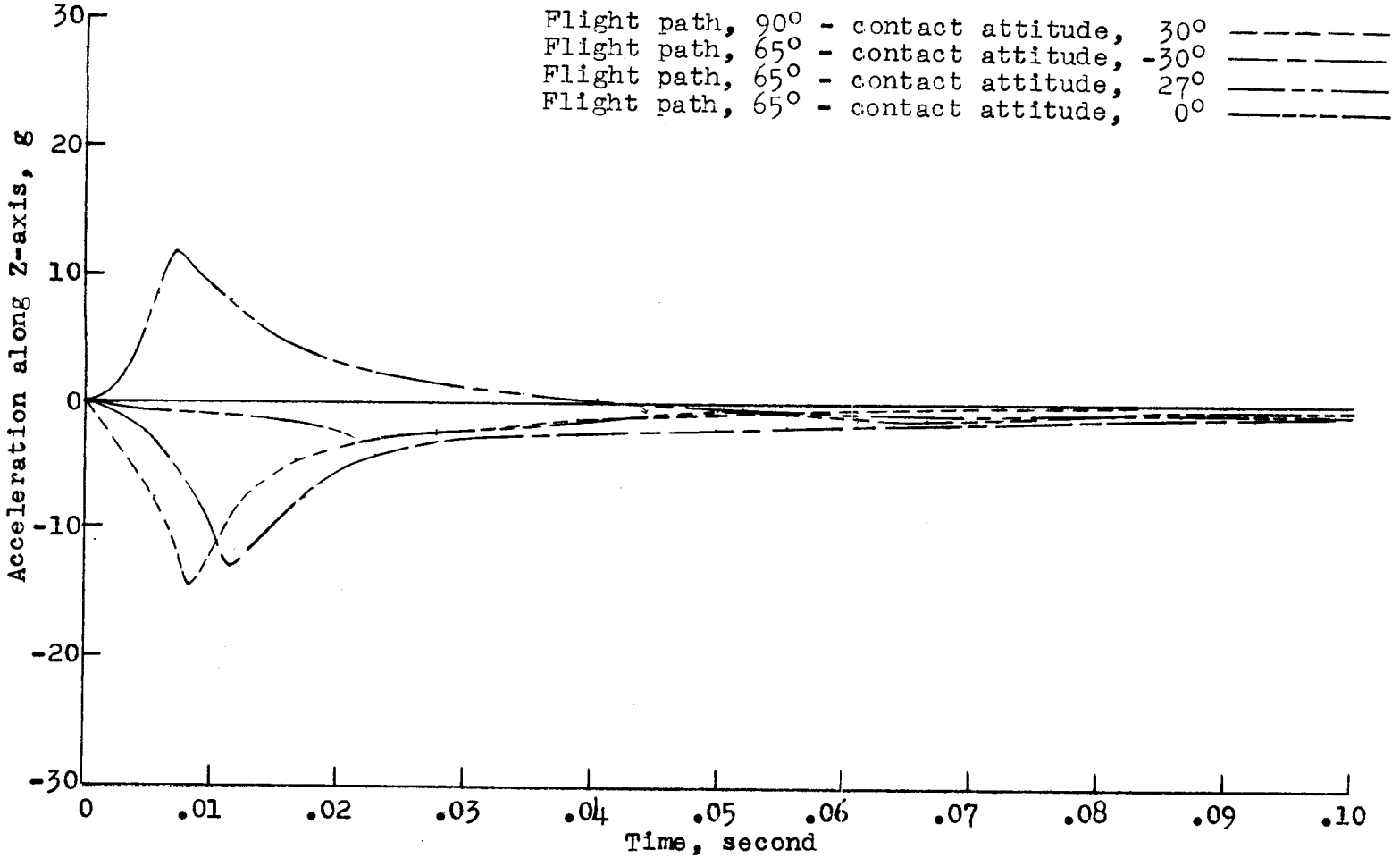

(c) Model C.

Figure 5.- Concluded.

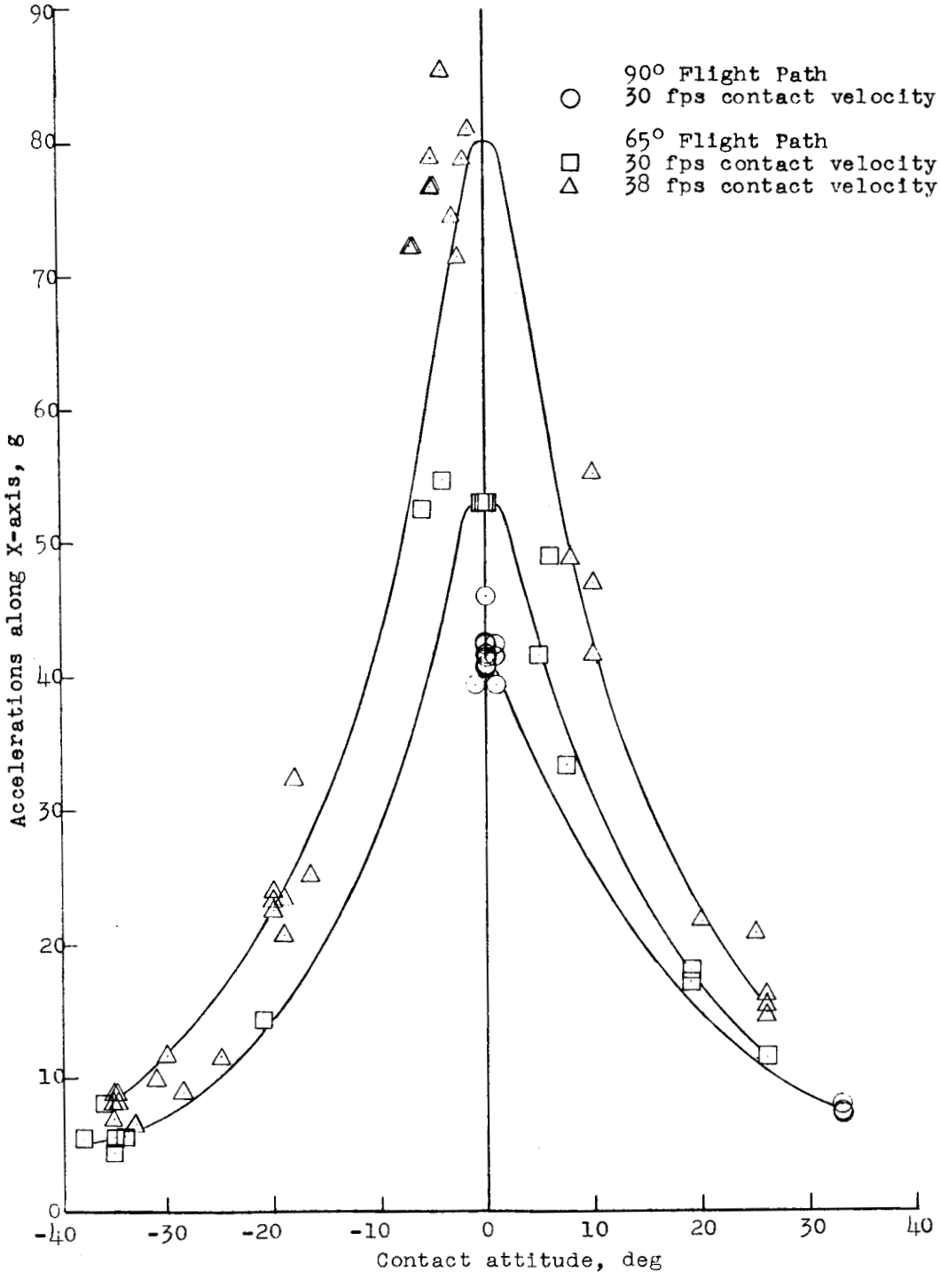

Figure 6.- Maximum accelerations along the X-axis of model A. All values are full scale.

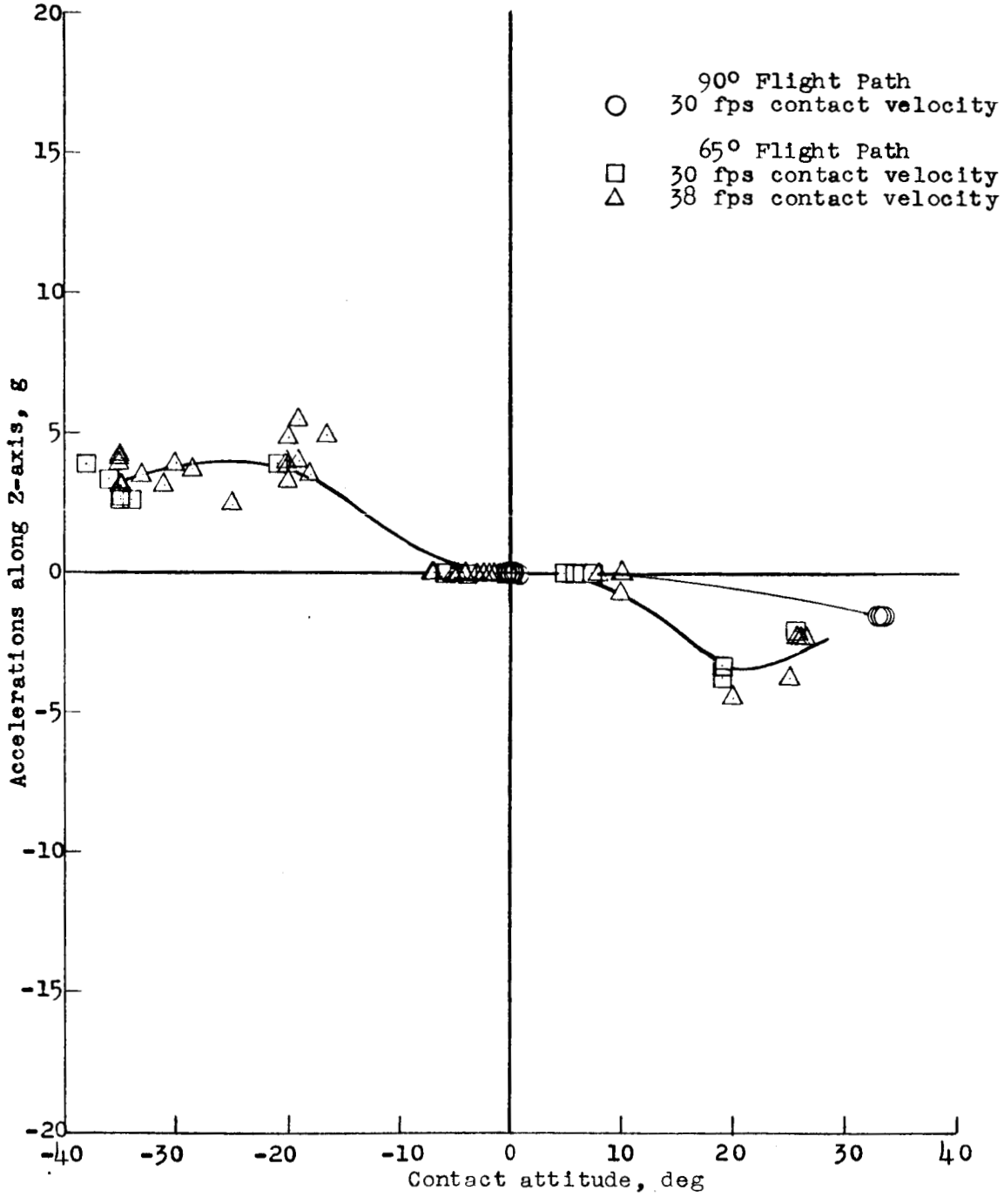

Figure 7.- Maximum accelerations along the Z-axis of model A. All values are full scale.

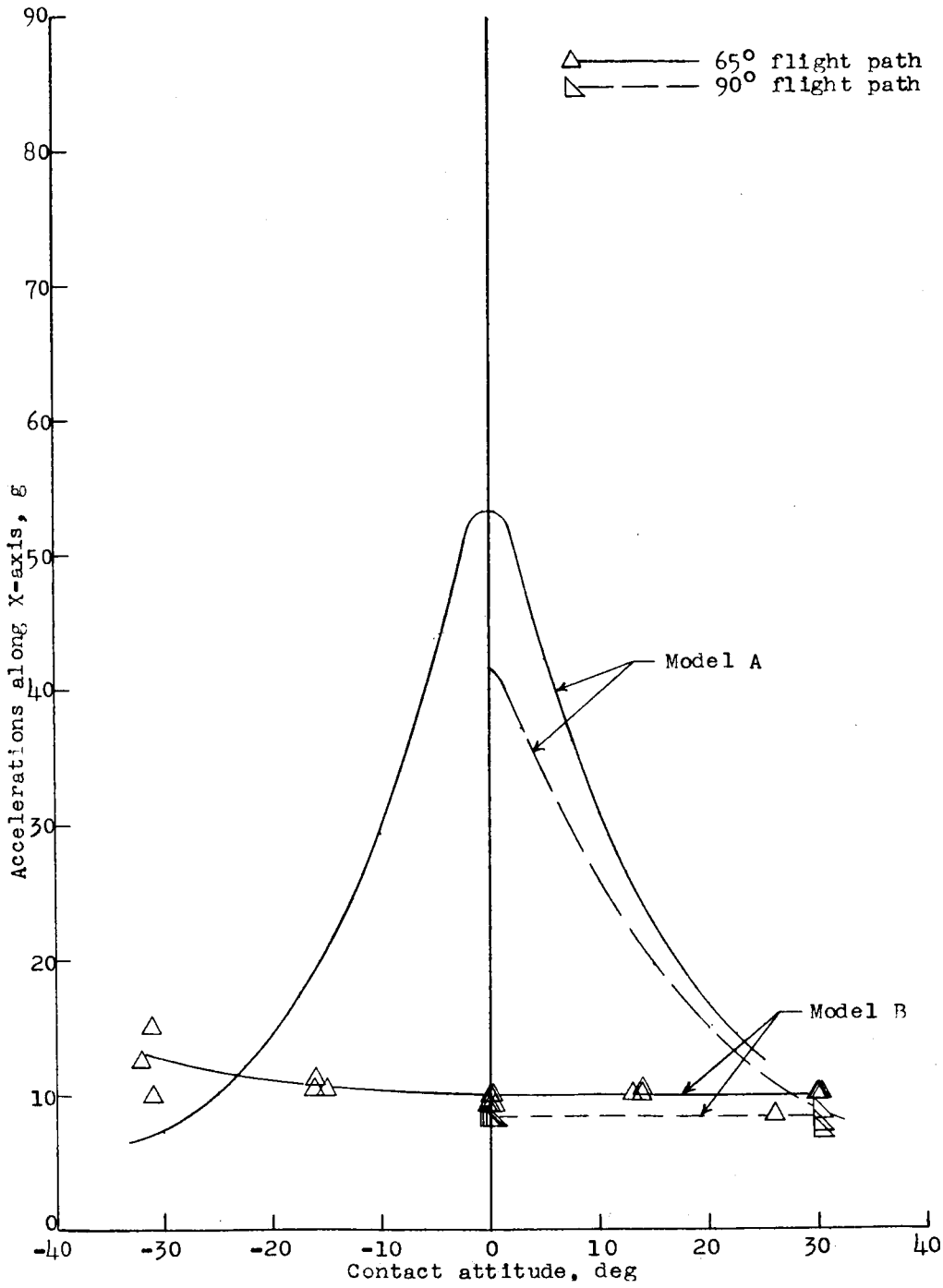

Figure 8.- Comparison of maximum accelerations along the X-axis of models A and B at a vertical contact velocity of 30 feet per second. All values are full scale.

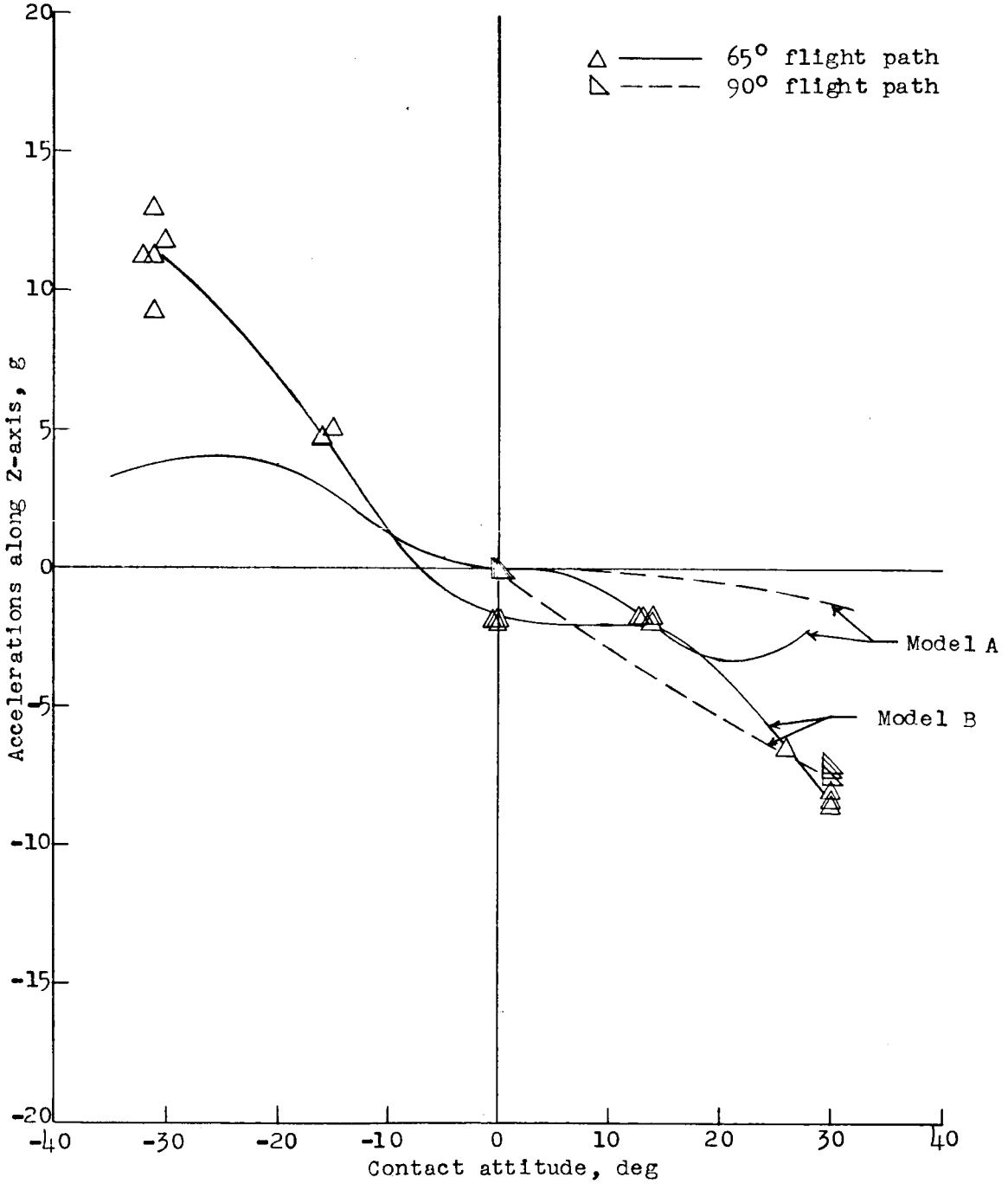

Figure 9.- Comparison of maximum accelerations along the Z-axis of models A and B at a vertical contact velocity of 30 feet per second. All values are full scale.

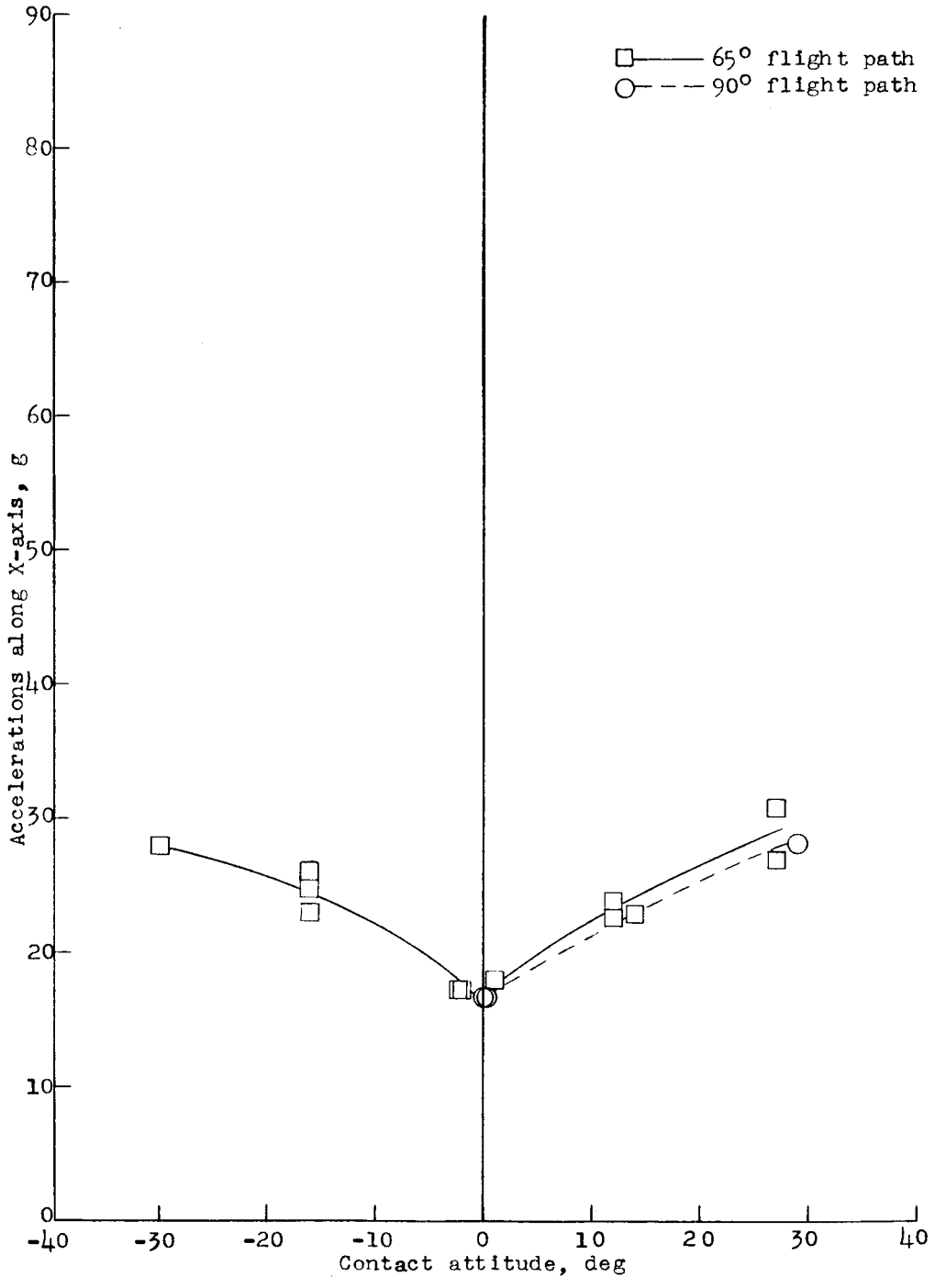

Figure 10.- Maximum accelerations along the X-axis of model C at a vertical contact velocity of 30 feet per second. All values are full scale.

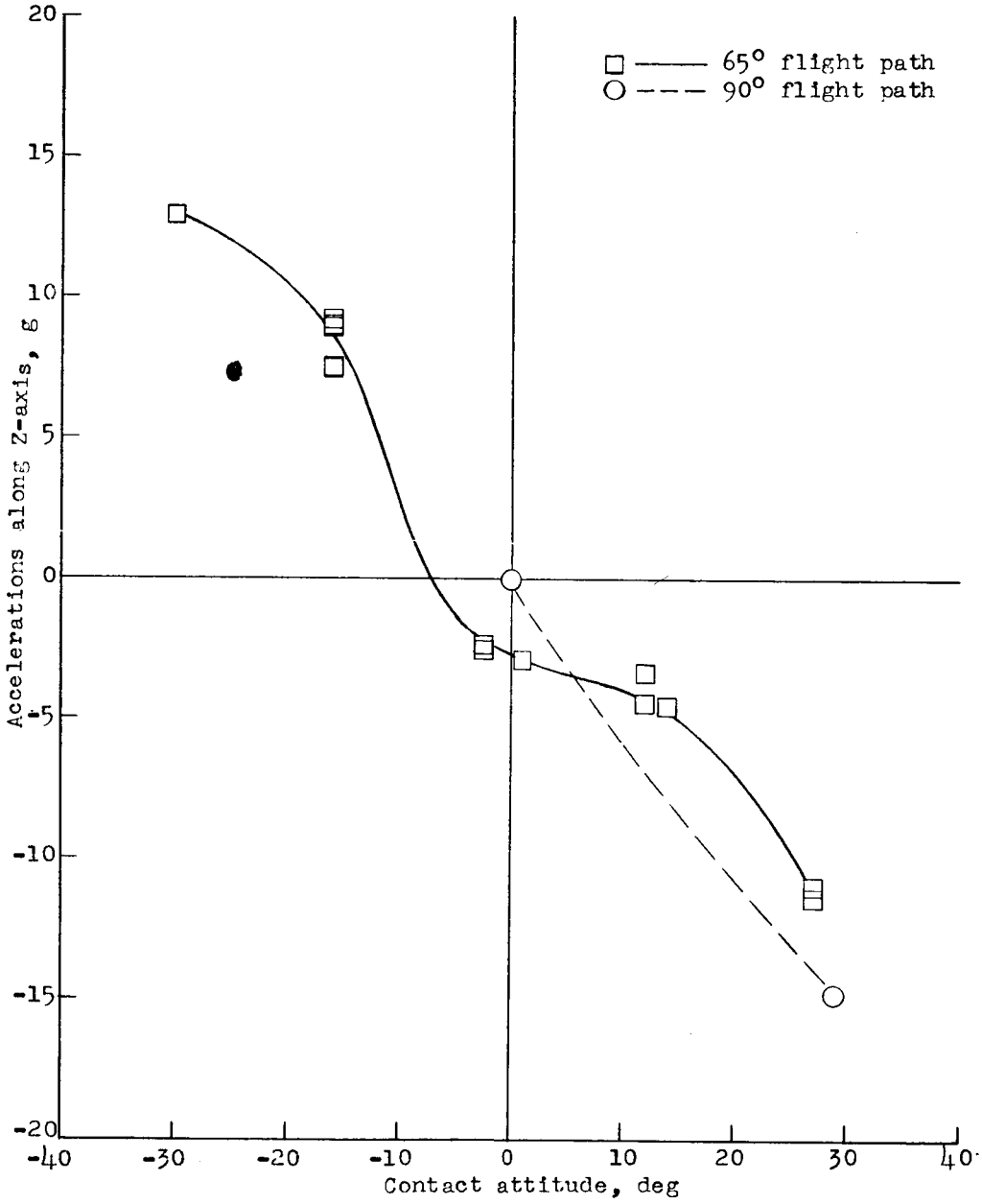

Figure 11.- Maximum accelerations along the Z-axis of model C at a vertical contact velocity of 30 feet per second. All values are full scale.

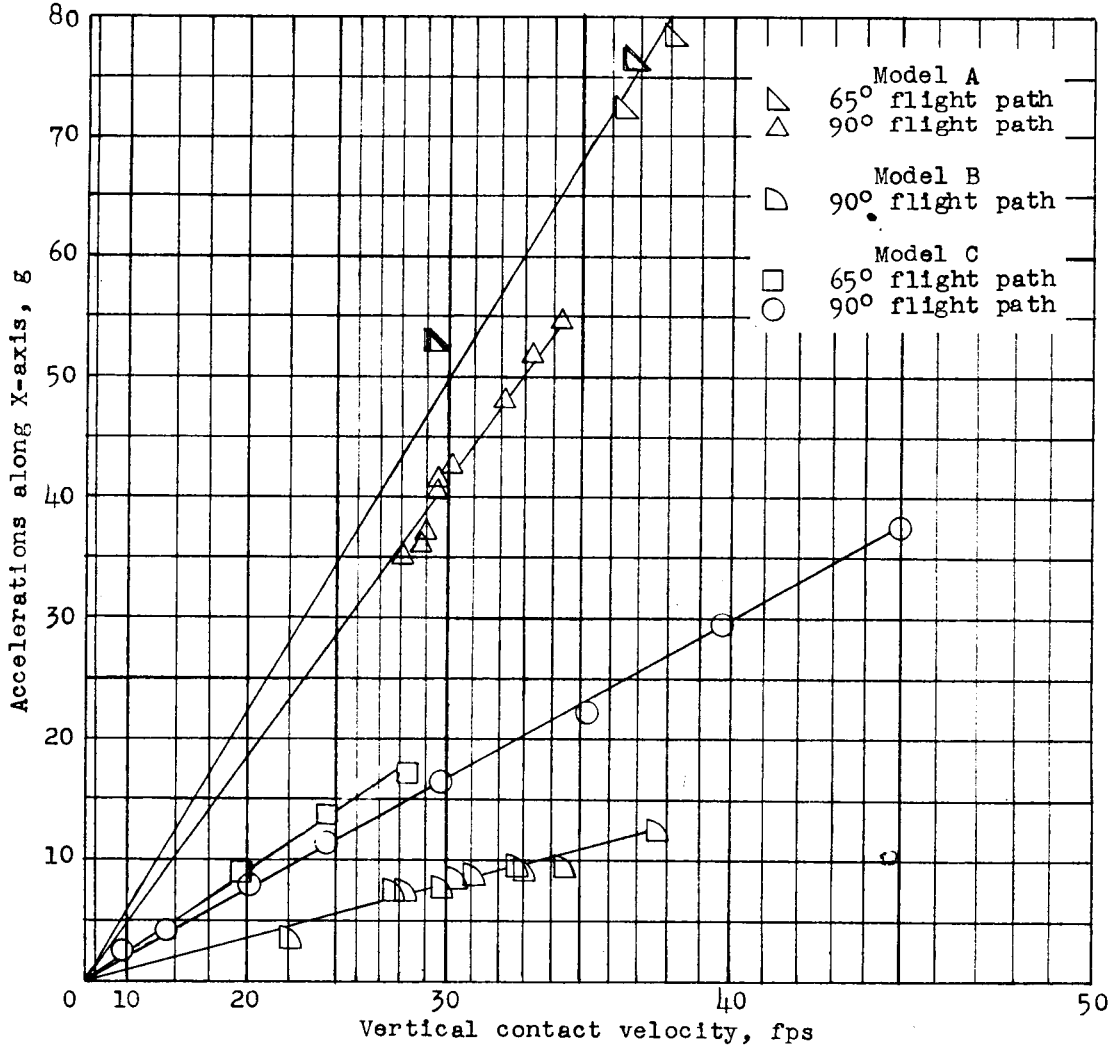

Figure 12.- Effect of contact velocity on accelerations along the X-axis of models A, B, and C at a contact attitude of 0°. All values are full scale.

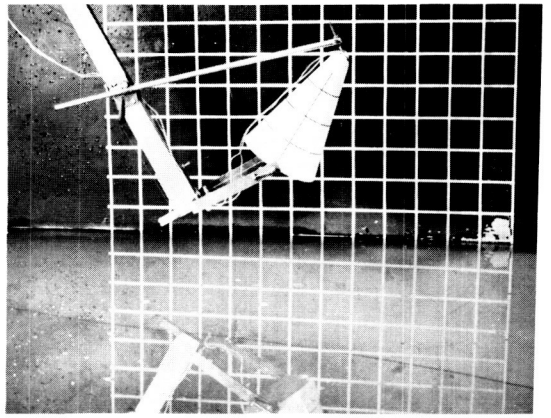

(a) Before contact.

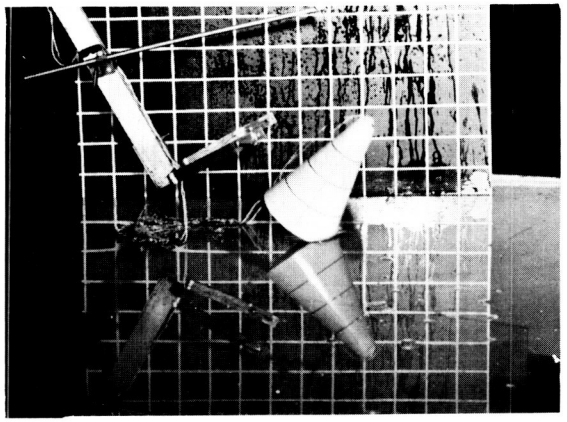

(b) 0.01 second after contact.

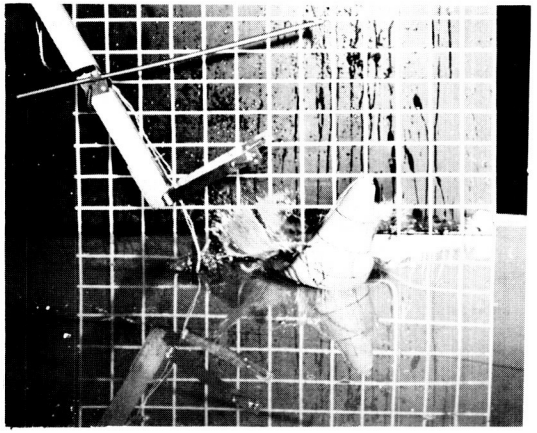

(c) 0.15 second after contact.

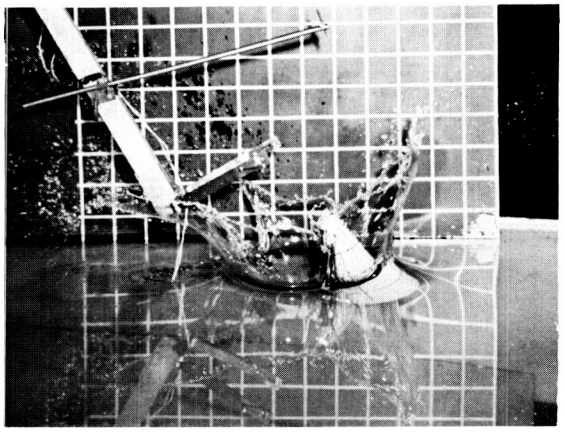

(d) 0.48 second after contact.

L-59-5015

Figure 13.- Sequence photographs showing a typical landing of model A from a 65° flight path at a -30° contact attitude and a vertical velocity of 30 feet per second. All values are full scale.

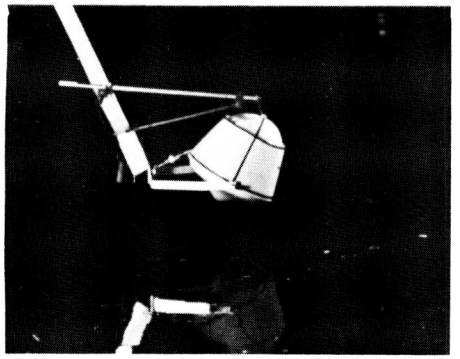

(a) Before contact.

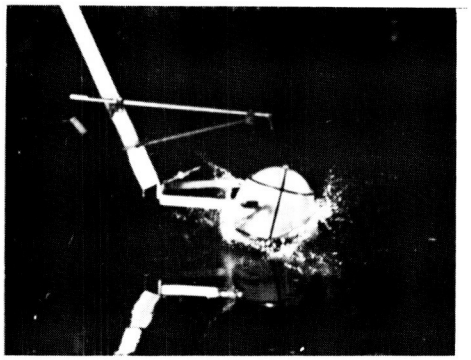

(b) 0.07 second after contact.

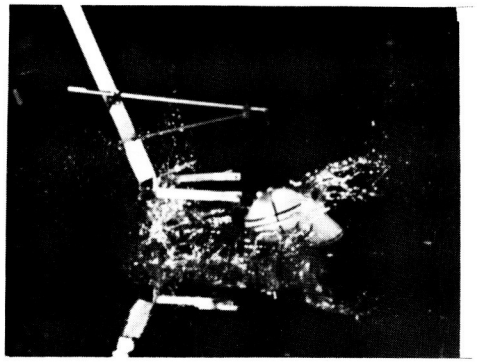

(c) 0.23 second after contact.

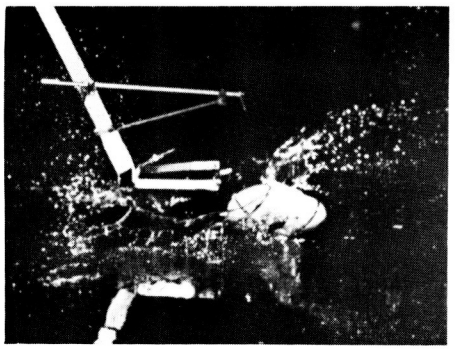

(d) 0.44 second after contact.

(e) 0.85 second after contact.

(f) 0.97 second after contact.

L-59-5016

Figure 14.- Sequence photographs showing a typical landing of model C from a 65° flight path at a -30° contact attitude and a vertical velocity of 30 feet per second. All values are full scale.

NASA - Langley Field, Va. L-540

L-540